INTRODUCTION OF A HIGH-LEVEL, APPLICATION BASED SIZING METHODOLOGY FOR CARNOT BATTERIES

Robin Tassenoy[1]*, Kenny Couvreur[1] , Wim Beyne[1], Michel De Paepe[1,2] , Steven Lecompte[1,2]

[1]Ghent University, Department of Electromechanical, Systems and Metal engineering, Ghent, Belgium

[2]FlandersMake @ UGENT, Core lab EEDT-MP, Leuven, Belgium

*Corresponding Author: Robin.Tassenoy@UGent.be

ABSTRACT

Due to the ever increasing share of renewable energy sources (RES) in the energy mix, large-scale energy storage systems are considered essential to ensure the security of supply in energy systems. In recent years, Carnot batteries have been introduced as an alternative grid-scale electrical storage system. In this storage concept, electrical energy is converted into heat, the heat is stored in a thermal storage system and finally converted back into electricity when needed. One of the main branches in the technology development is based on Rankine-cycles. The organic Rankine cycle (ORC) has potential for integration as the heat-to-power technology in this overall storage system. However, it is not clear how to size the system and assess its economic feasibility taking into account variable electricity production, demand and pricing. A sizing methodology based on a high-level generalized model of a Carnot battery is introduced to fill this gap. The methodology is explained in general and illustrated by a case study of load shifting of solar PV-panels for a non-residential university building with a high capacity of solar production.

1 INTRODUCTION

The growth of renewable energy requires flexible, low-cost and efficient electrical storage to balance the mismatch between energy supply and demand. Pumped hydro storage, compressed air energy storage, flow batteries and electrochemical cells are the commercially available large-scale energy storage technologies (European Commission, 2016). However, these technologies suffer from geographical constraints (such as pumped hydro storage and compressed air energy storage), require fossil fuel streams (like compressed air energy storage) or are characterized by a low lifespan (flow batteries and electrochemical cells). There thus is the need for new large-scale energy storage technologies, which do not suffer of the abovementioned drawbacks (Argyrou *et al.*, 2018).

Carnot batteries are a novel storage concept that could potentially fulfil these needs. The storage concept involves three steps. First, electrical energy is converted into heat using a heat pump or joule heater. Secondly, the heat is stored. Finally, a heat engine technology is used to convert the heat back to electricity when needed. In the literature, different alternatives for the power-to-heat, thermal storage and heat-to-power systems have been considered. In the literature, the power ratings of the thermal machines refer to the electrical input or output power respectively. The storage capacity of the Carnot battery refers to the electrical storage capacity except if the thermal storage capacity of the thermal energy storage system is referred to explicitly. This convention will be followed in this paper.

In the most simple system, an electrical resistive heater is used for the power-to-heat conversion. In this case the overall efficiency of the system is severely affected by the low heat-to-power efficiency of available heat engine technologies. Therefore, more complex heating systems are introduced based on heat pump technology. Two main branches exist: Brayton-based and Rankine-based systems. Typically, the same cycle type is used for the heat-to-power conversion. In this paper, focus will be given to Rankine-based systems. Three main branches can be distinguished: subcritical systems based on steam-

technology, subcritical systems based on ORC-technology and systems based on transcritical cycles. For an exhaustive discussion of the different types, the reader is referred to the review paper of Dumont *et al.* (2020).

The studies cited in this review paper all include a steady-state analysis and focus on the obtainable round-trip efficiencies of different system topologies. The sizing of the system is chosen arbitrarily with electrical power outputs ranging from 1 MW to 100 MW and storage durations ranging from 2 to 8 h. The choice for a specific power rating and charging/discharging duration is not elaborated upon. Moreover, the economics corresponding with the sizing of the system are mostly not taken into account.

In the context of the current study, systems based on ORC-technology are of main interest. Therefore, the terms heat pump and power-to-heat system can be used interchangeably, as can the terms ORC, heat engine and heat-to-power system. Only a few papers available discuss the sizing and economic aspects of these ORC-based systems.

Frate *et al*. (2020) studied a Carnot battery concept based on the use of heat pumps and ORCs from a thermo-economic point of view. The studied system is thermally integrated. This means low-grade thermal energy is used as additional energy input to the system, in order to improve the electric performance. Ten system parameters have been optimized for a simultaneous optimization of round-trip efficiency and system investment cost. The sensitivity of this optimization to the heat source, the nominal power rating of the heat pump and the storage duration (defined based on the charging time at nominal power) has been discussed. It has been assumed the charging and discharging time of the system is equal. Therefore, the nominal power of the ORC is a function of the heat pump power, system round-trip efficiency and storage duration. Cost scaling laws have been defined for round-trip efficiencies comprised between 0.5 and 0.9, for source temperatures between 70 and 80°C, for nominal heat pump power comprised between 500 and 5000 kW and for electrical storage capacities between 2000 and 40000 kWh. The choice for a heat pump range from 500 to 5000 kW and charging times from 4 to 8h has not been elaborated upon.

Hu *et al.* (2021) did a similar techno-economic optimization of a thermally integrated Carnot battery. The system parameters have optimized for a simultaneous optimization of round-trip efficiency and levelized cost of storage (LCOS). Five typical heat sources have been considered. The heat input by the heat source is fixed a priory. The system size is dictated by the available heat input, rather than the desired storage of electrical energy in the electric grid.

In both studies mentioned above, the system cost is related to its size. Only steady-state operation is analyzed. System parameters are optimized for the constant boundary conditions applied. The size ranges considered are not elaborated upon. For the LCOS-calculation by Hu *et al.* (2021) perfect daily charging/discharging cycles and constant electricity pricing have been assumed. The sizing of the system taking variable electricity production, demand and pricing into account has not been found in literature.

This study aims to fill this gap. A sizing methodology based on a high-level model of a Carnot battery is introduced that can be used for a primary system sizing in such a dynamic setting. The system itself is characterized by general performance parameters without any assumptions about the specific system lay-out. If the performance parameters of a specific lay-out and the related investment costs are known, the methodology introduced here can be used to select the optimal system size and to assess the economic feasibility of its implementation for a given electricity production, demand and price profile. As such, the sizing framework is generally applicable for different use cases and system topologies. The methodology will be demonstrated by a case study of load shifting of solar PV-production for a non-residential university building in Belgium. First, the model itself will be discussed. Then the specific case study will be introduced and the economic feasibility and system size will be analyzed.

2 MODEL DESCRIPTION

2.1 Model introduction

A high-level Python model has been developed to optimize the size of the Carnot battery for a given application. The aim is to determine the most optimal size of the different subsystems. It is assumed the thermodynamic performance of the subsystems is known from a previous analysis. The goal is thus not to make a detailed system model of the Carnot battery itself, but rather to get a first impression of the sizing of a known system in a variable environment. A schematic overview of the methodology is shown in Figure 1.

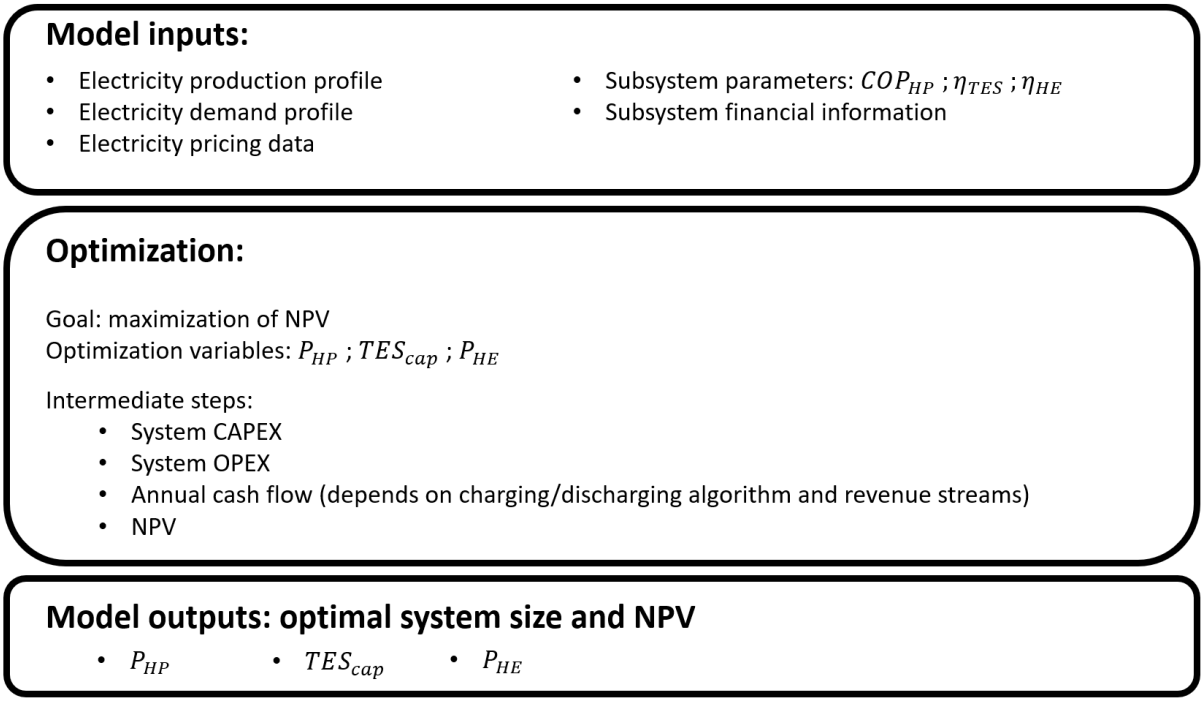

Figure 1: schematic overview of the optimization model

2.2 Input Data

The input data is used to introduce the operational conditions and the system characteristics to the model.

The operational conditions are mainly determined by the electricity production profile and the electricity demand profile that should be matched by the Carnot battery. Two arrays containing the amount of electricity produced and demanded in each timestep are thus used. In order to take economic considerations into account, an array with the variable electricity pricing corresponding with these production and demand profiles is used.

General system parameters are used to characterize the system of interest. The main performance parameters are the coefficient of performance of the heat pump (COP_{HP}), the efficiency of the thermal storage (η_{TES}) and the efficiency of the heat engine (η_{HE}). Next to the thermodynamic performance, economic aspects related to the system size should be quantified. The specific investment costs (CAPEX) and operational costs (OPEX) corresponding to the Carnot battery topology of interest are assumed to be known. If the specific costs are not know in detail, cost estimates of the different subsystems from literature can be used to make a first estimate of the costs.

2.3 System model

A high-level model of a Carnot battery is considered. The system consists of three building blocks: the power-to-heat system, the thermal energy storage system and the heat-to-power system. An overview of the subsystems and the energy flows in between is given in Figure 2.

The power-to-heat system is characterized by its COP. A COP equal to one corresponds with an electrical joule heater, while a higher COP could be obtained with a heat pump (HP). The thermal energy storage system (TES) is characterized by its storage efficiency (η_{TES}). The heat engine (HE) is characterized by its thermal efficiency (η_{HE}). The system's round-trip efficiency is given by equation (1) (Dumont *et al.*, 2020).

$$\eta_{RT,th} = COP_{HP} * \eta_{TES} * \eta_{HE} \tag{1}$$

The goal of the optimization model is to determine the optimal system size. The heat pump size is characterized by its electrical power rating P_{HP} (MW). The thermal storage system is characterized by its thermal capacity TES_{cap} (MWh_{th}). The heat engine is characterized by the electrical output power P_{HE} (MW).

The system is also characterized by its charging and discharging strategy. In general, this charging/discharging strategy can be adapted to the operation of interest. The current operation strategy aims at integrating as much as possible RES-electricity into the grid.

First, the difference between the electricity production and demand is calculated for each timestep.

$$E_{NP} = E_{production} - E_{demand} \tag{2}$$

If this net production (NP) is positive, the excess electricity production available will be used to charge the system. If the net production is negative, thermal energy will be extracted from the TES and electricity will be produced by the heat engine. During charging, the net production power is compared to the maximum power of the heat pump. If the net production power is higher or equal to this maximum power, the system will run at maximum power. If not, the system power is set equal to the available excess power. Part-load behavior is not considered and the COP is assumed constant. Once the charging power is determined, it is verified the free capacity of the TES is sufficient to store the heat corresponding with charging at this power during the timestep. This heat added to the TES during the timestep is related to the charging power by equation (4). If the state-of-charge (SOC) of the storage is not sufficiently high, the maximum power which result at a completely charged TES at the end of the timestep is used for charging. This is expressed by equation (5).

$$P_{NP} = \frac{E_{NP}}{\Delta t} \tag{3}$$

$$Q_{HP} = E_{NP} * COP_{HP} = P_{charge} * COP_{HP} * \Delta t \tag{4}$$

$$P_{charge} = \begin{cases} \min(P_{NP}, P_{HP}) & TES_{SOC,end} < 1 \\ \frac{TES_{cap} * (1 - TES_{SOC,start})}{COP_{HP}} & TES_{SOC,end} = 1 \end{cases} \tag{5}$$

During discharge a similar procedure is used. First, the net production power is compared to the maximum heat engine power. Depending on this comparison, the heat engine will function at full or part-load. The heat engine efficiency is assumed constant. The thermal energy extracted from the TES during the timestep is calculated by equation (6). If the thermal energy in the TES is not sufficient to run the heat engine at this power, the discharge power is reduced and the TES will be completely discharged at the end of the timestep. The discharge power is thus selected according to equation (7).

$$Q_{HE} = \frac{E_{HE}}{\eta_{HE}} = \frac{P_{discharge}}{\eta_{HE}} * \Delta t \tag{6}$$

$$P_{discharge} = \begin{cases} \min(|P_{NP}|, P_{HE}) & TES_{SOC,end} > 0 \\ TES_{cap} * TES_{SOC,start} * \eta_{HE} & TES_{SOC,end} = 0 \end{cases} \tag{7}$$

As no assumptions on the actual system lay-out (used cycles, storage temperatures,…) are made in this general model, dynamic and part-load characteristics are currently neglected. Performance of the components is assumed constant and an immediate response of the system in each timestep is used. If the part-load performance curve and response times of the specific topology are known, the modelling framework can be extended to take these into account.

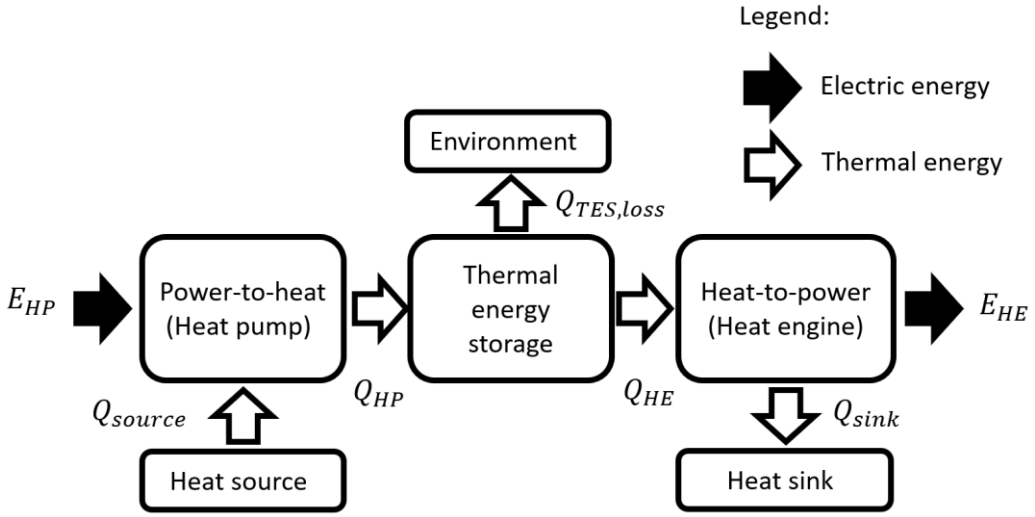

Figure 2: Overview of the system model and energy flows during charging and discharging

To simplify the interpretation of the results, the system size can be normalized taking the production and demand profile into account. The power of the heat pump and heat engine are normalized based on the maximum and minimum net production power respectively.

$$P_{HP,rel} = \frac{P_{HP}}{P_{NP,max}} \qquad P_{HE,rel} = \frac{P_{HE}}{|P_{NP,min}|} \tag{8}$$

The thermal capacity of the TES can also be expressed as a charging or discharging duration.

$$TES_{dur,charge} = \frac{TES_{cap}}{P_{HP} * COP_{HP}} \qquad TES_{dur,discharge} = \frac{TES_{cap}}{\frac{P_{HE}}{\eta_{HE}}} \tag{9}$$

The mismatch between supply and demand can be quantified by calculating the yearly overproduction and yearly underproduction over the year. The yearly overproduction is defined as the sum of all excess energy in the timesteps with a net production larger than 0. The yearly underproduction is defined as the sum of all energy shortages in the timesteps with a net production smaller than 0 (Equation (10)). The total energy charged and discharged by the Carnot battery can be normalized with respect to these maximum values (Equation (11)).

$$E_{overproduction} = \sum_{t=1}^{n} E_{NP} \;\; if \; E_{NP} > 0 \qquad E_{underproduction} = \sum_{t=1}^{n} |E_{NP}| \;\; if \; E_{NP} < 0 \tag{10}$$

$$E_{charged,rel} = \frac{E_{charged}}{E_{overproduction}} \qquad E_{discharged,rel} = \frac{E_{discharged}}{E_{underproduction}} \tag{11}$$

2.4 Economic performance evaluation

Economic considerations play an important role when evaluating potential investment decisions. The net present value (NPV) of an investment is considered the most comprehensive and complete criterion for investment decisions. It considers the time value of money, the total lifetime of the project and the cash flow (Lecompte, 2016). The NPV can be calculated as:

$$NPV = \sum_{t=1}^{n} \frac{CF}{(1+r)^t} - I_0 \tag{12}$$

In which I_0 represent the investment cost of the system, r the discount rate, n the system lifetime and CF the annual cash flow of the system. To evaluate the investment the annual cash flow compares the situation with investment to the situation without investment (Jacob *et al*., 2021):

$$CF = (revenue)_t - OPEX_t - CAPEX_t - R_t \tag{13}$$

The revenue is calculated as the profit made by the investment compared to the situation without investment and should thus be adapted to the specific use case of interest. Furthermore, the operational expenses (OPEX), reoccurring capital expenses ($CAPEX_t$) and the recovery value (R_t) of components with a longer lifetime than the time period considered are taken into account.

If the $NPV > 0$ the investment results in added value. If the $NPV < 0$ the investment results in a financial loss compared to the base situation. If $NPV = 0$ there is neither financial loss or gain.

The investment cost I_0 is clearly dependent on the topology of the Carnot battery considered. In order to get representative results, specific investment costs corresponding with the lay-out of interest should be used. The investment costs used to illustrate the optimization model will be explained in the case study section.

The annual cash flow is determined by the revenue-model corresponding with the studied application and should therefore be adapted to the case study at hand.

2.5 Optimization method

This study aims to optimize the system size in order to maximize the net present value (NPV) of the final system for a given set of input variables, while respecting certain bounds of the variables and assuring a certain level of RES-integration is obtained. In general, this can be written as:

$$\begin{cases} f(x) = \max(NPV) \\ x = \left[P_{HP}\ , TES_{cap}, P_{HE}\right]\ x \subseteq R \end{cases} \tag{14}$$

in which R represents the range of decision variables shown in Table 1.

Table 1: Ranges and constraints during optimization

Item	Symbol	Constraints
Heat pump power	P_{HP}	$[0\ ;\ P_{NP,max}]$
TES capacity	TES_{cap}	$[0\ ;\ \max(E_{overproduction}, E_{underproduction})]$
Heat engine power	P_{HE}	$[0\ ;\ \lvert P_{NP,min} \rvert]$

Currently, a brute force optimization approach is applied. The ranges shown in Table 1 are discretized and the performance of all combinations is evaluated and saved. Despite being more numerically intensive than dedicated optimization algorithms, this approach is currently used as it allows to analyze how the combination of system sizes influences the final performance.

3 CASE STUDY

Ghent University has committed to an ambitious energy policy plan (UGhent, 2019a). One of the main pillars is the compensation of the energy consumption by own renewable energy generation of all buildings build after 2009. One of these buildings, the IGhent-tower, has solar PV-panels to offset the electricity consumption of the building. At the moment, the electricity production of the solar panels present is insufficient (UGhent, 2019b). Future additions to the solar production have been planned in order to reach self-provision of the electricity demand by 2050. In the most favorable case, the total annual production by the solar panels should thus be equal to the total annual electricity consumption

of the building to reach the goal of the energy policy plan. In this study, the potential integration of a Carnot battery in this future scenario is evaluated.

3.1 Operational conditions

The electricity demand is simulated using a synthetic load profile for the year 2019 published by the system operator of the Belgian grid (VREG, 2019). This is a dataset which represents the electricity consumption during each quarter hour of the year relative to the total annual consumption. It takes the yearly calendar (weekdays, weekends and holidays, time of sunrise and down, etc.) into account. In this study, an S12-profile is used which is representative for non-residential users with a grid connection >56 kVA and is representative for the building considered.

The electricity production of the solar panels is simulated using a model developed by Laveyne *et al.* (2020). This model simulates the yield and production curve of decentralized solar panels placed in the low-voltage distribution grid, depending on the panel orientation and the irradiation data. Laveyne *et al.* used irradiation data distributed under license of the Belgian Royal Meteorological Institute, which cannot be made freely available. The authors developed a novel "all-sky distribution" model to take the contribution of diffuse irradiation on the PV-panel into account. The model developed is suitable for the Belgium irradiation profile. Based on the total irradiance, the power output of a typical solar PV-panel is calculated. Finally, the authors developed an inverter model to calculate the useful AC-production of the solar panels. In the current study, the most optimal orientation given the Belgian irradiation data is assumed, which corresponds with an azimuth of 0 degrees and a tilt angle of 34.5 degrees.

The electricity production and demand profile are shown for one year in Figure 3 (a). In Figure 3 (b) the evolution is shown in more detail for one summer week. To simplify the interpretation of these figures, both the electricity production and demand have been normalized with the maximum electricity production over the year. From these figures it can be seen that the variation of the solar production is significantly higher than the variation of the demand. For the non-residential user considered, the electricity consumption during the weekend (days 187 and 188) is significantly lower than on weekdays. An important note to make is that the demand profiles used are representative for the time before the COVID19-pandemic. Due to the pandemic, a lot of people work from home and the energy use is likely to be slightly lower on weekdays as well.

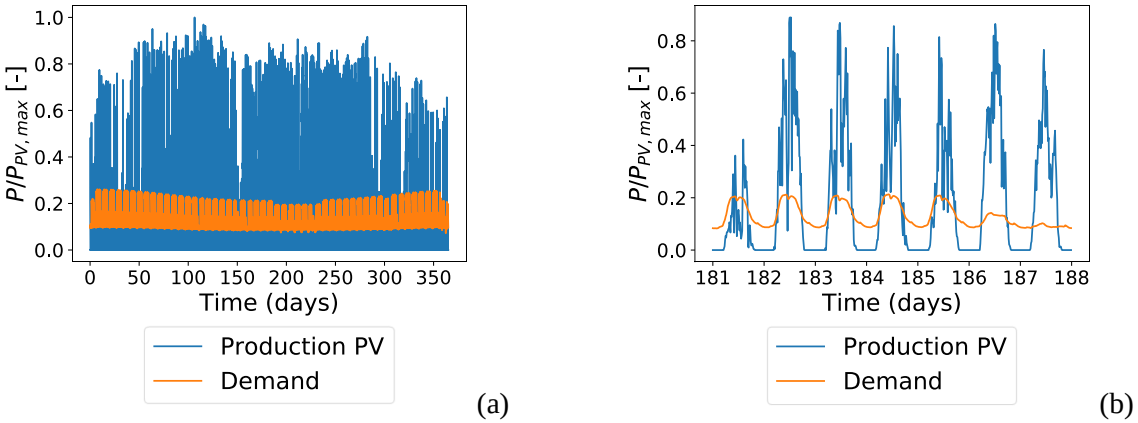

Figure 3: Normalized production and demand profiles for one year (a) and one week (b).

The yearly electricity demand of the considered University building equals approximately 2600 MWh/year (UGhent, 2019b). As explained before, a possible future scenario in which the yearly production of solar panels equals this demand is evaluated. For the production and demand profiles used, the absolute net production values used for the normalization of the results are summarized in table 2.

Table 2: normalization values for the case study

Parameter	Value	Parameter	Value
$E_{overproduction}$	1505 MWh	$P_{NP,max}$	1.85 MW
$E_{underproduction}$	1505 MWh	$\lvert P_{NP,min} \rvert$	0.55 MW

3.2 Subsystem performance parameters

In this study, the performance of a Carnot battery using ORC-technology is of interest. To get reasonable estimates for the input values of the performance parameters of the heat pump and the ORC depending on the operational conditions, these parameters will be calculated with respect to the efficiency of a Carnot cycle operating in the same conditions. It is assumed that the heat pump operates between a source temperature T_{source} and a fixed temperature of the thermal storage T_{TES}. The ORC operates between the same T_{TES} and the sink temperature T_{sink}. This is a simplification of reality as it neglects the pinch points of the heat exchangers, thermal stratification in the TES and variation of the storage temperature dependent on the state-of-charge of the TES. Nevertheless, this approach is found to be accurate enough for the current high-level sizing. The performance parameters of the system can thus be written as:

$$COP_{HP} = \eta_{HP,II} * \frac{T_{TES}}{T_{TES} - T_{source}} \tag{15}$$

$$\eta_{HE} = \eta_{HE,II} * \left(1 - \left(\frac{T_{sink}}{T_{TES}}\right)\right) \tag{16}$$

In the IGhent-tower, a datacenter is able to provide significant amounts of waste heat. Depending on the cooling technology used, captured waste heat temperatures vary from 25°C to 35°C for air-cooled and between 50°C and 60°C for liquid submersion-cooled datacenters (Wahlroos, 2017). Therefore, a source temperature of 50°C is assumed. It is assumed the ambient air is used as heat sink. The yearly average ambient temperature in Belgium is 10.6°C (KMI, 2020). This value will thus be used as sink temperature. Arpagaus *et al*. (2018) made a literature review on large-scale (very) high temperature heat pumps, which could be interesting for application in a Carnot battery. Delivery temperatures of 90°C to 160°C have been found. They found delivery temperatures up to 100°C are commercially available. Therefore a TES-temperature of 100°C has been selected. This temperature is well within the operational limits of pressurized water sensible storage systems (IEA ECES, 2018). For vapour compression and vapour recompression heat pumps, $\eta_{HP,II} = 0.5$ is considered a reasonable estimate (van de Bor and Infante Ferreira, 2013). Based on the efficiencies of ORCs in operated in the desired power and temperature range, a similar $\eta_{HE,II}$ can be found (Öhman and Lundqvist., 2013). A value of $\eta_{HE,II} = 0.5$ is used. According to McTigue *et al.* heat losses can be reduced to negligible values with sufficient insulation. Self-discharge of the storage is thus neglected and an η_{TES} equal to 1 is used.

3.3 Economic considerations

To make an estimate of the investment costs of the system, investment costs of the different subsystems have been searched in literature. The specific investment costs of the subsystems found in literature are summarized in Table 3.

Table 3: specific CAPEX-estimates for the different subsystems

Subsystem	CAPEX-estimate	Reference
Heat pump	1900 EUR/kW_{el}	Berenschot *et al.*, 2015
TES	20.5 EUR/kWh_{th}	IEA ECES, 2018 (Industrial pressurized hot water storage, temperature range 80-140°C)
Heat engine	4216 EUR/kW_{el}	Lemmens, 2016

All these price estimates have been converted to the reference year 2019, using the composite cost index approach (Lemmens., 2016). The cost indices are based on the chemical engineering cost index (Olympios *et al.*, 2021). The system lifetime is assumed to be 25 years, the discount rate r 5% the

operational expenses are calculated as 1.5% of the total investment cost per year and the reoccurring CAPEX and recovery value are assumed to be 0 (Hu *et al*., 2021).

It is assumed the solar panels are already available. These are thus not included in the investment costs. In the situation without Carnot battery, no electricity has to be bought in periods of overproduction. However, as no storage is present, in periods of underproduction the total demand should be bought from the grid at the instantaneous prices. In the situation with Carnot battery, the excess electricity in periods of overproduction can be used to charge the Carnot battery without additional costs. In periods with underproduction, the Carnot battery can be discharged. As such less electricity has to be bought from the electricity grid at these periods, leading to annual savings.

4 RESULTS

A summary of the optimal system sizes to reach a certain level of RES-integration is simulation given in Table 4. It can be seen all NPV-values found are negative, indicating that the implementation of a Carnot battery in this particular case study is never feasible.

The maximal NPV has been found for the smallest system size tested by the brute force approach. The additional integration of RES by installing this system is rather small, as only 15% of the overproduction is charged by the system. Only 7% of the annual shortage is delivered by the Carnot battery. The optimal system sizes to charge 50, 75, 90 and almost 100% of the annual overproduction are listed in Table 4 as well. An increasing amount of electricity charged and discharged corresponds with lower NPV. At higher amounts of electricity charged the marginal cost increases. A trade-off between economic feasibility and integration of RES is observed.

If only the integration of RES is considered, it can be seen that the power of both the heat pump and ORC can be reduced significantly for a modest reduction in energy charged and discharged over the year. In the economically most optimal solution to reach a certain $E_{charged,rel}$, the charging times are systematically lower than the discharging times.

In future work, the sensitivity of the obtained results to the assumed costs and system efficiencies should be analyzed in depth. Moreover, detailed thermo-economic analysis of different topologies could improve the accuracy of the NPV-estimate and allow to compare the economic feasibility of different system lay-outs for this particular case study.

Table 4: summary of optimum system sizes and NPV, dependent on the minimum $E_{charged,rel}$

$P_{HP,rel}$ [-]	$P_{HE,rel}$ [-]	$TES_{dur,charge}$ $[h]$	$TES_{dur,discharge}$ $[h]$	NPV [EUR]	$E_{charged,rel}$ [-]	$E_{discharged,rel}$ [-]
0.1	0.1	4.4	6.6	$-7.82 * 10^5$	0.15	0.07
0.3	0.2	5.8	13.2	$-2.13 * 10^6$	0.50	0.22
0.4	0.4	9.8	14.8	$-3.50 * 10^6$	0.75	0.34
0.6	0.4	14.5	33.3	$-5.26 * 10^6$	0.90	0.40
0.8	0.5	32.7	79.0	$-9.65 * 10^6$	0.996	0.45

5 CONCLUSIONS

A high-level model to assess the economic feasibility and optimal system size based on the intended system use has been presented. The methodology has been discussed in general and illustrated by a case study. The use of a Carnot battery based on ORC-technology for load-shifting of solar PV-production of a university building. For this specific case, no economic feasible system size has been found. A trade-off between economic feasibility and higher levels of RES-integration has been observed. The sensitivity of the obtained results to the assumed system costs and efficiencies will be analyzed in depth in future work.

REFERENCES

Arpagaus, C., Bless, F., Uhlmann, M., Schiffmann, J., 2018, High temperature heat pumps: Market overview, state of the art, research status, refrigerants, and application potentials, *Energy*, vol. 152: p. 985-1010.

Argyrou, M.C., Christodoulides, P., Kalogirou, S.A., 2018, Energy storage for electricity generation and related processes: Technologies appraisal and grid scale applications, *Renew. Sust. Energ. Rev.*, vol. 94: p. 804–821.

Berenschot, CE Delft, ISPT, 2015, Power to Products Over de resultaten, conclusies en vervolgstappen, Available at: https://www.topsectorenergie.nl/sites/default/files/uploads /Eindrapport_Power_to_Products_externe_link.pdf [accessed 28.06.2021]

Dumont, O., Frate, G.F., Pillai, A., Lecompte, S., De Paepe, M., Lemort V., 2020, Carnot battery technology: A state-of-the-art review, *J. Energy Storage*, vol. 32: 101756.

European Commission, 2016, Clean energy for all Europeans

Frate, G.D., Ferrari, L., Desideri, U., 2020, Multi-Criteria Economic Analysis of a Pumped Thermal Electricity Storage (PTES) With Thermal Integration, Front. Energy Res., vol.8:53.

Ghent University (UGhent), 2019a, Energy policy plan 2020-2030: the road for Ghent University in the energy transition, Available at: https://www.ugent.be/nl/univgent/waarvoor-staat-ugent/duurzaamheidsbeleid/leidraad/energie-2/energiebeleidsplan.pdf [accessed 30.06.2021]

Ghent University (UGhent), 2019b, Electricity demand and solar PV production of the IGhent-tower Available at: https://ugent.erbisweb.be/GraphPage.aspx?buildingCode=UG60330109 [accessed at 30.06.2021]

Hu, S., Yang, Z., Li, J., Duan, Y., 2021, Thermo-economic analysis of the pumped thermal energy storage with thermal integration in different application scenarios, *Energy Convers. Manag.*, vol. 236: 114702.

International Energy Agency ECES Annex 30, 2018, Applications of thermal energy storage in the energy transition benchmarks and developments, Available at: https://www.eces a30.org/wp-content/uploads/Applications-of-Thermal-Energy-Storag-in-the-Energy Transition-Annex-30-Report.pdf [accessed 28.06.2021]

Jacob, R., Riahi, S., Liu, M., Belusko, M., Bruno, F., 2021, Technoeconomic Impacts of Storage System Design on the Viability of Concentrated Solar Power Plants

KMI, 2020, Belgian climate, https://www.meteo.be/nl/klimaat/klimaat-van-belgie/ klimatologischoverzicht/2019/jaar [accessed 30.06.2021]

Laveyne, J., Bozalakov, D., Van Eetvelde, G. and Vandevelde, L., 2020, Impact of Solar Panel Orientation on the Integration of Solar Energy in Low-Voltage Distribution Grids, *Int. J. Photoenergy*, vol. 2020: Article ID 2412780.

Lecompte, S., 2016, Performance evaluation of organic Rankine cycle architectures: application to waste heat valorization, Ghent Belgium: p. 23-27.

Lemmens, A., 2016, Cost Engineering Techniques and Their Applicability for Cost Estimation of Organic Rankine Cycle Systems, *Energies*, vol.9: 485.

McTigue, J.D., White, A., Markides, C.N., 2015, Parametric studies and optimization of pumped thermal electricity storage, *Appl. Energy*, vol. 137: p. 800-811.

Öhman, H., Lundqvist, P., 2013, Comparison and analysis of performance using Low Temperature Power Cycles, *Appl. Therm. Eng.*, vol. 52: p. 160-169.

Olympios, A.V., McTigue, J.D., Farres-Antunez, P., Tafone, A., Romagnoli, A., Li, Y., Ding, Y., Steinmann, W.-D., Wang, L., Chen, H., Markides, C.N., 2021, Progress and prospects of thermo-mechanical energy storage-a critical review, *Prog. Energy*, vol. 3: 022001

van de Bor, D.M., Infante Ferreira, C.A., 2013, Quick selection of industrial heat pump types including the impact of thermodynamic losses, *Energy*, vol. 53: p. 312-322.

Vlaamse Regulator van de Elektriciteits- en Gasmarkt (VREG), 2019, Synthetic Load Profiles- Available at: https://www.vreg.be/nl/verbruiksprofielen [accessed 19.02.2021]

Wahlroos, M., Pärssinen, M., Manner, J., Syri, S., 2017, Utilizing data center waste heat in district heating – Impacts on energy efficiency and prospects for low-temperature district heating networks, *Energy*, vol.140: p.1228-1238.